SUSCEPTIBILITY, ECHO TIME SHIFTS, AND T2* CONSIDERATIONS FOR FUNCTIONAL MAGNETIC RESONANCE IMAGING

Bradley P. Sutton, Yue Zhuo

Bioengineering Department, University of Illinois at Urbana-Champaign, Urbana, IL

ABSTRACT

Magnetic susceptibility differences exist near the interface of air/tissue in the ventral brain in fMRI (functional magnetic resonance imaging). These susceptibility differences will not only cause field inhomogeneity and its gradients which will result in image artifacts, but also cause shifts in the echo time for gradients echo acquisitions. The echo time shifts are caused by shifts in the effective k-space trajectory due to the gradients of the field inhomogeneity. Previous work has shown and validated methods for estimating the echo time shift based on the effective k-space trajectory. In this work, we demonstrate that accurate estimation of the R2* decay map (R2*=1/T2*) not only need to account for the field map and its gradients, but also needs to include the echo time shift. These changes in T2* sensitivity are directly related to changes in sensitivity in BOLD (blood oxygenation level dependent) fMRI studies.

Index Terms— Echo time shift, Field inhomogeneity, Magnetic susceptibility, BOLD fMRI

1. INTRODUCTION

Accurate spatial localization in magnetic resonance imaging relies on a uniform main magnetic field in the absence of imaging gradients. However, due to differences in the magnetic properties of tissue and air, non-uniformities in magnetic field exist when a sample or subject is placed in the MRI scanner. Tissue and air have different magnetic susceptibility, a property that denotes the magnetizability of a substance.

The resulting magnetic field inhomogeneity can cause a variety of artifacts during imaging. These artifacts depend on the type of sequence, gradient-echo versus spin-echo, and the timing of the acquisition. Both spin echo and gradient echo imaging methods suffer from image distortions due to magnetic susceptibility. These image distortions can result in geometric shifts in image along phase encode axis if an echo planar acquisition is used [1] or blurring in spiral acquisitions [2]. These distortions are well studied and many correction methods exist to correct the image if a measured field map is available. Pixel shift methods can be used for EPI acquisitions [1, 3-5] and conjugate phase methods can correct non-Cartesian, spiral acquisitions [6-8].

Besides image distortion effects that rely on the value of the magnetic field at each pixel location, there are two other magnetic susceptibility effects that are due to gradients in magnetic field distribution. These affect gradient echo acquisitions which are frequently used in functional MRI (fMRI) applications. In a 2D acquisition, gradients of the magnetic field in *slice direction* will cause signal loss in acquired image. If we assume a rectangular profile for the selected slice with slice thickness of Δz, the image intensity of a pixel with a susceptibility gradient of Z (in rad/s per pixel) will decay approximately as:

$$\left| I(\mathbf{r}_n) \right| \cong \left| \tilde{I}(\mathbf{r}_n) \right| sinc(Z_n T_E I(2\pi)) , \qquad (1)$$

where $\left| \tilde{I}(\mathbf{r}_n) \right|$ would be the intensity of the image pixel at location $\mathbf{r}_n$ without the gradient in the through-slice direction. Note that the signal intensity at the echo time, T_E, determines the overall scaling of the image and the bulk contrast. Several methods have been proposed to address through-plane dephasing and signal loss including reducing the slice dimension [9-11], z-shimming [12], external shims [13], and tailored RF pulses [14-16].

Finally, the gradients in the magnetic field distribution in the *in-plane directions* can cause effective k-space shifts [17-19]. This can induce several artifacts resulting from local variations in the sample density of k-space shifts [19] that are large enough that the signal intensity for a voxel was not adequately sampled [18]. In addition to these effects that result in loss of image quality, in this paper we focus on the changes in echo time that can result in improper contrast in the resulting images and improper inferences based on the functional data.

Fig 1. Field map gradients effects on effective echo time shift in gradient echo acquisition

As shown in Fig.1, gradients in the in-plane directions will cause k-space and echo time shifts that are dependent on exact spatial location, the magnetic susceptibility properties of the surrounding regions, and the quality of the shimming procedure in the local area. The blood
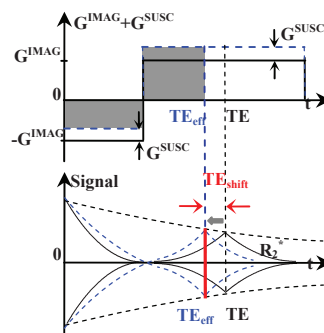
oxygenation-level dependent (BOLD) fMRI signal is dependent upon the echo time. Local changes in echo time will affect the sensitivity of the fMRI experiment to detect changes in these regions. Additionally, bulk changes between two examined populations that result in systematic macroscale susceptibility differences may result in systematic differences in sensitivity between the two groups in a study.

In this abstract, we will examine errors in estimated T_2^* values as a function of shimming using several image reconstruction options on spiral-out gradient echo data. We will examine standard gridding, field-inhomogeneity reconstruction based on conjugate phase [6], and an advanced iterative reconstruction that includes a model of linear gradients in the field map [20-21].

2. THEORY

In this section, we will first briefly mention about effective k-space trajectory, then explain the concept of the echo time shift and the reason for this shift exist based on the analysis of the effective k-space trajectory.

2.1. k-space based approach

Without loss of generality, we can consider only the effect of a gradient in the magnetic field inhomogeneity in the x-direction. The additional gradient in a voxel due to the magnetic susceptibility creates an effective k-space trajectory that deviates from the intended imaging trajectory. The effective trajectory can be found by integrating the net gradient, which is given by,

$$G_x^{TOT}(\mathbf{r}) = G_x^{IMAG} + G_x^{SUSC}(\mathbf{r}) , \qquad (2)$$

where $G_x^{TOT}(\mathbf{r})$ is the net gradient in the voxel at position $\mathbf{r}$, G_x^{IMAG} is the applied imaging gradient in the x-direction (same for every voxel), and $G_x^{SUSC}(\mathbf{r})$ is the gradient in the magnetic susceptibility induced field map in the x-direction at voxel position $\mathbf{r}$ (different for every voxel). This results in a k-space trajectory that is spatially dependent as shown in Fig. 2. The susceptibility gradients will cause an effective echo time change in gradient-echo acquisitions, such as those discussed in [21].

Let us first introduce the notion of shift in the echo time. For a spiral-out trajectory in k-space, Fig.2 (a) shows the one dimensional effective k-space trajectory in x-direction. The second and third curve with shading, $G_{SUSC,\alpha}$ and $G_{SUSC,\beta}$, represent the additional gradient induced by the magnetic susceptibility in x-direction before and during the data acquisition, respectively; The forth to sixth curves (k^{IMAG}, k^{SUSC}, and $k^{IMAG} + k^{SUSC}$) represents the original k-space trajectory in x-direction (k^{IMAG}), the corresponding additional k-space trajectory due to magnetic susceptibility gradients (k^{SUSC}), and the over all effective k-space trajectory in x-direction ($k^{IMAG} + k^{SUSC}$), which introduces a

shift in echo time. The echo time is defined as the time at which the central portion of k-space is sampled.

Fig.2 (b) shows the two dimension (2D) effective k-space trajectory with susceptibility gradients in x-direction. The first figure represents the original 2D k-space trajectory without susceptibility gradients; the second and third figures represent the 2D k-space trajectory due to the susceptibility gradients before and during the data acquisition, respectively; the forth figure represents the over all effective 2D k-space trajectory correspondingly, and we can see clearly that the k-space center is shifted out from the origin of the original 2D k-space.
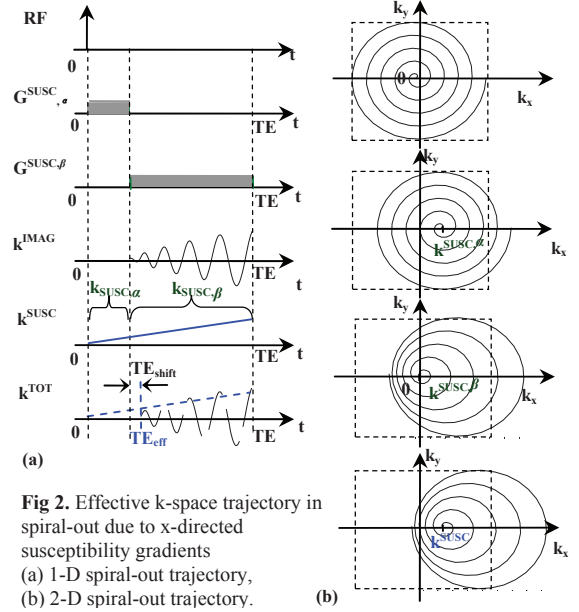

Fig 2. Effective k-space trajectory in spiral-out due to x-directed susceptibility gradients
(a) 1-D spiral-out trajectory,
(b) 2-D spiral-out trajectory.

The echo time represents the peak time of the echo which occurs when the center of k-space is sampled. Thus the echo time will be shifted due to the existence of the susceptibility gradient in gradient echo acquisition.

2.2. Effect of susceptibility gradients on signal model

In order to account for the susceptibility degradations, we include in the signal model the effects of the magnetic field distribution and its first-order gradients. As shown in Equation (3), the k-space signal model with the effective k-space is (for m=1, … , M):

$$S(\mathbf{k}(t_m)) = \Phi(\mathbf{k}(t)) \sum_{n=1}^{N} f(\mathbf{r}_n)e^{-i\omega(\mathbf{r}_n)t_m}e^{-i2\pi\mathbf{k}_m\mathbf{r}_n} , \qquad (3)$$

where $S(\mathbf{k}(t))$ is the k-space signal, $f(\mathbf{r})$ is the image intensity at position $\mathbf{r}$ in image space. $\mathbf{k}_m$ is the imaging k-space trajectory ($\mathbf{k}^{IMAG}$). $\omega(\mathbf{r}_n)$ is the field map which can be expanded with gradients with piece-wise linear model, where the field map gradients results $\mathbf{k}^{SUSC}$ (due to magnetic susceptibility gradients, which will cause echo time shift). N is the number of pixels and M is the number of data points in k-space; (Δ_x, Δ_y) is the dimension of voxel. And $\Phi(\mathbf{k}(t))$

is the Fourier transform of the voxel indicator function, i.e. $sinc(\Delta_x k_x(t)+G_{Xn}t_m/2\pi)$ $sinc(\Delta_y k_y(t) +G_{Yn}t_m/2\pi)$ $sinc(\Delta_z k_z(t)+ +G_{Zn}t_m/2\pi)$. We apply this model to iterative reconstruction with conjugate gradients to correct for the geometric distortion, signal loss and echo time shift.

3. METHODS

In this section, we first describe the experimental setting used to acquire the data and obtain a measurement of the field map. Then we present the procedure used to estimate effective echo time based on the effective k-space trajectory. Thereafter, we compare the different R2* maps estimated with or without the effective echo time. Note that R2* is the inverse of T2*. Finally, we present the reconstruction technique used to account for the echo time shift.

The experimental data was acquired on a Siemens Allegra 3 T headscanner. The parameters of the scan were: matrix size 64x64, FOV 24 cm, 20 slices, slice thickness 5 mm, TR 4 s. Data acquisition was obtained using a multiecho, 2D single-shot spiral-out trajectory while the field map was estimated from a multiecho acquisition using a multishot spiral-out trajectory (12 shots). A multishot trajectory was chosen to ensure accuracy of the field map estimate. The field map was smoothed prior to its use in estimation/reconstruction steps. The echo times of the multiecho acquisition were 2.5 ms + (0, 1, 20, 40) ms. We use a slice that is very far from the major air/tissue interfaces in the ventral brain to show that even small gradients in the magnetic field distribution can drive significant errors in T2* estimation.

To calculate the echo time shifts, we use a method based on the effective k-space trajectory. Fig. 3 shows the image intensity as a function of the echo time for a given pixel. The main

Fig. 3 Image intensity as a function of the echo time (for a given pixel)

principle to estimate the TE shift is to calculate the minimum distance of the effective k-space trajectory from center to determine the point in the trajectory that cross zero. Once the echo time shift is estimated, it can be accounted for during estimation of the R2* map. We use a nonlinear curve-fitting algorithm to obtain the R2* map, using Equation (4):

$$I(r,T_E,T_{E,\text{shift}}) = \rho(r,T_E = 0)e^{-(T_E + T_{E,\text{shift}})R_2^*}, \quad (4)$$

where $I(r,T_E,T_{E,\text{shift}})$ represents reconstructed image intensity at echo time T_E with echo time shift $T_{E,\text{shift}}$, and ρ represents the image intensity with an echo time of 0 ms.

As mentioned earlier, the imaging model can be modified to account for the susceptibility using the magnetic field map gradients. We have studied several reconstruction methods to visualize the influence of both the field map gradients and the TE shift. First, a simple **gridding** method was applied with no compensation for the magnetic field map. Then, we use the **gridding method with field map** correction, using the conjugate phase method [6]. Finally, an **iterative algorithm** correcting for shifts in the effective k-space trajectory has been developed for comparison. This reconstruction is based on our previous work and not only the field map but also the gradients of the field map have been added in the signal formation imaging model.

4. RESULTS

In this section, we show that accurate estimation of R2* requires including both correction for susceptibility artifacts in the reconstruction and accounting for echo time shifts. We have compared the R2* signal decay map estimated using different reconstruction techniques with or without TE shift.

We have analyzed three different reconstruction techniques: (a) gridding, (b) gridding + FM, and (c) iterative as described above. Reconstructed images are then used to estimate the R2* map using Equation (4) and a curve fitting from different echo time values. The first row of Fig. 4 presents the estimated R2* map using the different reconstruction methods. The second row additionally introduces the TE shift in the curve fitting process used to obtain the R2* map. The resulting R2* maps are compared to a reference map estimated from a multishot trajectory (12 shots). We assume that the multishot image is less degraded by the susceptibility artifacts than single shot acquisitions. Fig. 5 shows the errors between each estimated R2* map previously presented and the reference R2* map.

The normalized root mean square error (NRMSE) between R2* map of each reconstruction method and the reference map is given in Table 1 (The mask for NRMSE excluded the region with fat contamination in the edge). The numerical values show that accounting for TE shift improves the quality of the estimated R2* map. As predicted, the best R2* map estimation is obtained when using an iterative reconstruction correcting for both field map and gradients of field map coupled with use of the effective TE values. Note that the NRMSE in (b) is slightly higher than in (a). This might be due to the relatively low field map values in the selected slice so the distortion is small and only field map correction does not help.

Table 1. Normalized root mean square errors in R2* estimate

	(a) Gridding	(b) Gridding + FM	(c) Iterative
NRMSE$_{TE}$	0.2787	0.2988	0.2300
NRMSE$_{TE\ eff}$	0.2620	0.2818	0.2206

In BOLD fMRI, a single R2*-weighted image is acquired at an echo time to optimize functional contrast and
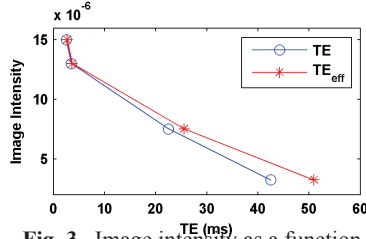
Signal-to-Noise Ratio (SNR). However, depending on gradients in the magnetic field map, this echo time can vary significantly across a functional image [22-23]. Accurate functional inferences must account for both image distortion effects and echo time shifts that result from the magnetic susceptibility differences in the brain.
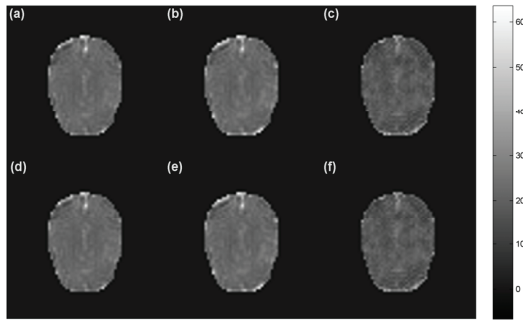

Fig. 4 Estimated R2* from several reconstructions using Nominal TE: (a) Gridding, (b) Gridding + FM, (c) Iterative; Effective TE: (d) Gridding, (e) Gridding + FM, (f) Iterative.
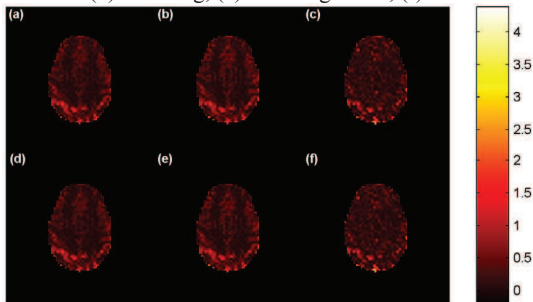

Fig 5. Errors of the reconstructed image verse the reference image Nominal TE: (a) Gridding, (b) Gridding + FM, (c) Iterative; Effective TE: (d) Gridding, (e) Gridding + FM, (f) Iterative.

5. CONCLUSION

Based on the analysis above, we conclude that the existence of the magnetic field inhomogeneity and the corresponding echo time shifts in gradient-echo data acquisitions will cause susceptibility artifacts affecting the image quality and functional imaging contrast with BOLD sensitivity. For improved accuracy of R2* estimation and BOLD signal, we not only need to correct for the magnetic susceptibility using the extended k-space signal model, including the physics of the field map and its gradients, but also need to correct for the echo time shifts induced by the susceptibility gradients during the image analysis and interpretation stages. Magnetic susceptibility can significantly affect estimate of R2* and BOLD sensitivity even in slices far from air/tissue interfaces where the field map and its gradients are small.

REFERENCES
[1] Sekihara, K., et al. Image restoration from non-uniform magnetic field influence for direct Fourier NMR imaging. *Physics Med Biol*, 1984. 29(1): p. 15-24.

[2] Yudilevich, E. et al. Spiral sampling in magnetic resonance imaging - the effect of inhomogeneities. *IEEE Trans Med Imaging*, 1987. 6(4): p. 337-345.

[3] Sumanaweera, T.S., et al. MR susceptibility misregistration correction. *IEEE Trans Med Im*, 1993. 12(2): p. 251-259.

[4] Jezzard, P. et al. Correction for geometric distortion in echo planar images from B0 field variations. *Magn Reson Med*, 1995. 34: p. 65-73.

[5] Reber, P.J., et al. Correction of off resonance-related distortion in echo-planar imaging using EPI-based field maps. *Magn Reson Med*, 1998. 39: p. 328-330.

[6] Noll, D.C., et al. A homogeneity correction method for magnetic resonance imaging with time-varying gradients. *IEEE Trans Med Imaging*, 1991. 10(4): p. 629-637.

[7] Man, L.C., et al. Multifrequency interpolation for fast off-resonance correction. *Magn Reson Med*, 1997. 37: p. 785-792.

[8] Schomberg, H. Off-resonance correction of MR images. *IEEE Trans Med Imaging*, 1999. 18(6): p. 481-495.

[9] Merboldt, K.D., et al. Reducing inhomogeneity artifacts in functional MRI of human brain activation-thin sections vs gradient compensation. *Journal of magnetic resonance*, 2000. 145(2): p. 184-191.

[10] Wadghiri, Y.Z., et al. Sensitivity and performance time in MRI dephasing artifact reduction methods. *Magn Reson Med*, 2001. 45(3): p. 470-476.

[11] Bellgowan, P.S., et al. Improved BOLD detection in the medial temporal region using parallel imaging and voxel volume reduction. *NeuroImage*, 2006. 29(4): p. 1244-1251.

[12] Glover, G.H. 3D z-shim method for reduction of susceptibility effects in BOLD fMRI *Magn Reson Med*, 1999. 42(2): p. 290-299.

[13] Hsu, J.J. et al. Mitigation of susceptibility-induced signal loss in neuroimaging using localized shim coils. *Magn Reson Med*, 2005. 53(2): p. 243-248.

[14] Ro, Y.M., et al. A new frontier of blood imaging using susceptibility effect and tailored RF pulses. *Magn Reson Med*, 1992. 28(2): p. 237-248.

[15] Stenger, V.A., et al. Three-dimensional tailored RF pulses for the reduction of susceptibility artifacts in T(*)(2)-weighted functional MRI. *Magn Reson Med*, 2000. 44(4): p. 525-531.

[16] Stenger, V.A., et al. Multishot 3D slice-select tailored RF pulses for MRI. *Magn Reson Med*, 2002. 48(1): p. 157-165.

[17] Maeda, A., et al. Reconstruction by weighted correlation for MRI with time-varying gradients. *IEEE Trans Med Imaging*, 1988. 7(1): p. 26-31.

[18] Reichenbach, J.R., et al. Theory and application of static field inhomogeneity effects in gradient-echo imaging. *J Magn Reson Imaging*, 1997. 7(2): p. 266-79.

[19] Noll, D.C., et al. Conjugate phase MRI reconstruction with spatially variant sample density correction. *IEEE Trans Med Imaging*, 2005. 24(3): p. 325-36.

[20] Sutton, B.P., et al. Compensating for within-voxel susceptibility gradients in BOLD fMRI, in *12th Soc. Magn. Reson. Med*. 2004. p. 349.

[21] Liu, G. et al. EPI image reconstruction with correction of distortion and signal losses *J Magn Reson Imaging*, 2006. 24(3): p. 683-9.

[22] Deichmann R., et al. "Compensation of susceptibility-induced BOLD sensitivity losses in echo-planar fMRI imaging," *Neuroimage*. 2002 Jan. 15(1): p.120-35.

[23] Zhuo, Y. et al. Effect on BOLD Sensitivity Due to Susceptibility-induced Echo Time Shift in Spiral-in Based Functional MRI, Submitted in IEEE EMBS 2009.